ACS APPLIED MATERIALS & INTERFACES

Research Article

www.acsami.org

Effect of Surface Wettability Properties on the Electrical Properties of Printed Carbon Nanotube Thin-Film Transistors on SiO_2/Si Substrates

Zhen Liu,[†,‡] Jianwen Zhao,*[,†] Wenya Xu,[†] Long Qian,[†] Shuhong Nie,[†] and Zheng Cui*[,†]

[†]Printable Electronics Research Centre, Suzhou Institute of Nano-Tech and Nano-Bionics, Chinese Academy of Sciences, No. 398 Ruoshui Road, Science and Education Innovation District (SEID), Suzhou Industrial Park, Suzhou, Jiangsu Province 215123, People's Republic of China

[‡]School of Materials Science and Engineering, Dalian Jiaotong University, Dalian, Liaoning Province 116028, People's Republic of China

Supporting Information

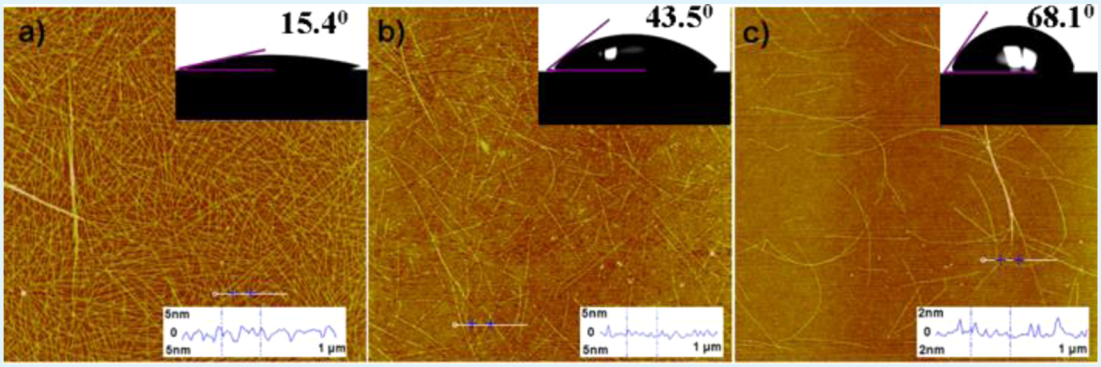

ABSTRACT: The precise placement and efficient deposition of semiconducting single-walled carbon nanotubes (sc-SWCNTs) on substrates are challenges for achieving printed high-performance SWCNT thin-film transistors (TFTs) with independent gates. It was found that the wettability of the substrate played a key role in the electrical properties of TFTs for sc-SWCNTs sorted by poly[(9,9-dioctylfluorene-2,7-diyl)-*co*-(1,4-benzo-2,1,3-thiadiazole)] (PFO-BT). In the present work we report a simple and scalable method which can rapidly and selectively deposit a high concentration of sc-SWCNTs in TFT channels by aerosol-jet-printing. The method is based on oxygen plasma treatment of substrates, which tunes the surface wettability. TFTs printed on the treated substrates demonstrated a low operation voltage, small hysteresis, high mobility up to 32.3 $cm^2 V^{-1} s^{-1}$, and high on/off ratio up to 10^6 after only two printings. Their mobilities were 10 and 30 times higher than those of TFTs fabricated on untreated and low-wettability substrates. The uniformity of printed TFTs was also greatly improved. Inverters were constructed by printed top-gate TFTs, and a maximum voltage gain of 17 at V_{dd} = 5 V was achieved. The mechanism of such improvements is that the PFO-BT-functionalized sc-SWCNTs are preferably immobilized on the oxygen plasma treated substrates due to the strong hydrogen bonds between sc-SWCNTs and hydroxyl groups on the substrates.

KEYWORDS: *printed thin-film transistors, sorted, single-walled carbon nanotube, wettability, electrical properties, uniformity*

INTRODUCTION

Recently, printable electronics have become a hot topic because large-area and flexible electronic systems can be produced at low cost.[1−7] Printed thin-film transistors (TFTs) are the key components in the fields of printed electronics, such as the backplane for displays, logic circuits, and artificial electronic skin.[8−19] With the advances in new materials and new process techniques, the electrical properties of printed TFTs, in particular, mobility and on/off ratio, have been gradually improving in the past few years; however, poor uniformity is still a critical issue in printed TFTs.

Commercial single-walled carbon nanotubes (SWCNTs) are a mixture of metallic and semiconducting species, and it is difficult to achieve TFTs with high mobility, high on/off ratio, and high yield if the metallic species are not selectively removed or eliminated from the SWCNTs prior to use. Various approaches, such as density gradient ultracentrifugation (DGU), polymer wrapping, and gel chromatography, have been developed to selectively remove or eliminate metallic species in commercial SWCNTs.[20−35] Among them, polymer wrapping has become one of the most valid methods to sort semiconducting SWCNTs (sc-SWCNTs) from commercial SWCNTs since Bao's work was published in 2011.[23] A number of studies using various polymers to selectively sort the sc-SWCNTs have been reported,[15,20−25,32] including the authors' work which demonstrated that the cheap and commonly used

Received: December 6, 2013
Accepted: June 16, 2014
Published: June 16, 2014

poly(9,9-dialkylfluorene) derivative poly[(9,9-dioctylfluorene-2,7-diyl)-*co*-(1,4-benzo-2,1,3-thiadiazole)] (PFO-BT) has the ability to sort sc-SWCNTs from commercial arc discharge SWCNTs.[15] However, transistors based on PFO-BT-sorted sc-SWCNTs showed low mobility (less than 5 $cm^2 V^{-1} s^{-1}$) even after 10 printings or drop-castings.

It is known that SWCNT inks contain different kinds of surfactants, polymers, and other additives to increase the solubility of SWCNTs and stability of SWCNT inks. However, all of them will increase the tube-to-tube junction resistances as well as carrier scattering centers, resulting in degradation of intrinsic electrical properties of SWCNTs. Solvent washing and annealing are commonly used to remove impurities and to improve the electrical properties of printed SWCNT TFTs. Unfortunately, sc-SWCNTs can also be removed together with impurities during the course of washing if the interaction between sc-SWCNTs and the substrates is too weak. The substrates are, therefore, commonly functionalized by (3-aminopropyl)triethoxysilane (APTES), poly-L-lysine, or 4-(*N*-hydroxycarboxamido)-1-methylpyridinium iodide (NMPI) to increase the adhesion between sc-SWCNTs and the substrates, resulting in an increase of the density of SWCNTs in the device channels and improvement in the electrical properties of SWCNT TFT devices.[36−39] However, we found that functionalization of substrates by APTES or poly-L-lysine may work well for aqueous-based sc-SWCNTs inks but has no positive effect for solvent-based sc-SWCNTs inks (as shown in Figure S1, Supporting Information). Instead, we found that a simple oxygen plasma treatment of the substrate can significantly improve the electrical properties of transistors based on PFO-BT-sorted sc-SWCNTs. The mobility of printed TFTs increased 10-fold when the substrates were treated by oxygen plasma for 1 min. The printed TFTs also showed good uniformity.

In this paper, sorting of sc-SWCNTs by PFO-BT has been characterized. High-wettability substrates obtained by oxygen plasma treatment have been investigated. TFTs have been fabricated by aerosol-jet-printing of PFO-BT-sorted sc-SWCNT ink, and their electrical properties have been measured. A low operation voltage, a small hysteresis, mobility in the range of 8.2−32.3 $cm^2 V^{-1} s^{-1}$, and an on/off ratio in the range of 10^6 to 10^8 have been achieved in the printed TFTs after only two printings. Inverters based on the printed top-gate SWCNT TFTs showed voltage gain up to 17 at V_{dd} = 5 V. Measurements of 200 printed TFTs have shown good uniformity in their electrical properties.

RESULTS AND DISCUSSION

UV−Vis−NIR Spectra and Raman Spectra of SWCNTs Sorted by PFO-BT. To demonstrate the ability of PFO-BT for selectively wrapping sc-SWCNTs over arc discharge SWCNTs, the supernatants were characterized by a PerkinElmer Lambda 750 UV−vis−NIR spectrometer. Figure 1 shows the typical adsorption spectra of sorted SWCNTs in xylene after centrifugation at 21000*g* for 1 h. As shown in Figure 1, the S_{22} semiconducting peaks in the range of 850−1300 nm became very sharp and the background very low after interaction with PFO-BT; at the same time, the M_{11} metallic peaks in the range of 600−800 nm can hardly be observed, which indicates the removal of the metallic species with the aid of sonication and centrifugation. The supernatant was used to directly fabricate TFTs by drop-casting or aerosol-jet-printing without any other purification.

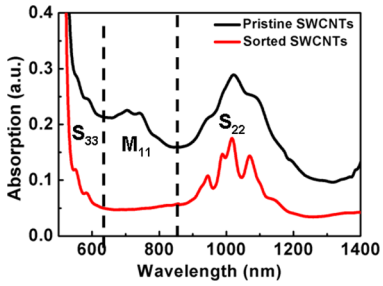

Figure 1. Adsorption spectra of SWCNTs sorted from arc discharge SWCNTs by PFO-BT in xylene after centrifugation at 21000*g* for 1 h.

To further verify the successful removal of metallic SWCNTs, the sorted SWCNT thin films were characterized by a confocal Raman microscope. According to the Kataura plot and the previous reports, a strong metallic peak at 163 cm^{-1} and a small metallic peak at 200 cm^{-1} can be observed under 785 and 633 nm lasers, respectively.[20,21,41,42] As shown in Figure 2a,b, the metallic peaks at 163 and 200 cm^{-1} disappear after the SWCNTs are sorted by PFO-BT with the aid of sonication and centrifugation. The G^- peak of sorted SWCNTs becomes very sharp, and the integrated area of the G^+/G^- ratio is much higher than that of pristine SWCNTs, indicating the selective removal of metallic species by PFO-BT (Figure 2d). In addition, parts b and c of Figure 2 show that sc-SWCNTs were selectively wrapped by PFO-BT. In brief, metallic species are selectively removed and the semiconducting species are preferentially sorted from arc discharge SWCNTs by PFO-BT in xylene with the aid of sonication and centrifugation.

Effect of the Wettability of Substrates on the Electrical Properties of Printed Sorted sc-SWCNT TFTs. It has been demonstrated that high-density sc-SWCNTs can be achieved on NMPI-modified substrates via the Coulombic bonding force between NMPI and sc-SWCNTs. However, once the SWCNTs are deposited, a high-temperature (450 °C) annealing is needed to remove the NMPI because the self-assembled monolayer has an adverse effect on the electrical properties of TFTs.[39] There are few reports on the relationship between the substrate wettability and the electrical properties of SWCNT TFTs besides our previous paper.[40] Here, the effect of the wettability of the substrates on the electrical properties of PFO-BT-functionalized SWCNT TFTs was investigated.

As shown in Figure 3, the untreated SiO_2/Si surface with a water contact angle of 43.5° can be changed to a high-wettability surface with a water contact angle of 15.4° after treatment with oxygen plasma (100 W) for 1 min or a low-wettability surface with a water contact angle of 68.1° after being annealed at 200 °C in a vacuum oven for 1 h. As-prepared sc-SWCNTs were deposited on three substrates with different water contact angles by drop-casting or aerosol-jet-printing followed by washing with xylene, and the electrical properties of the TFTs were then measured by using a Keithley 4200-SCS semiconductor parameter analyzer.

Figure 4 shows the typical transfer curves and the output curves of devices fabricated on three kinds of substrates with different water contact angles. It is evident that all devices can work well and show high on/off ratios ranging from 10^5 to 10^8, and the mobilities of devices fabricated on three different substrates with water contact angles of 15.4°, 43.5°, and 68.1° are 26.6, 2.23, and 0.94 $cm^2 V^{-1} s^{-1}$. It is noted that the mobility of devices fabricated on high-wettability substrates is 10 times and 30 times higher than those on the other two

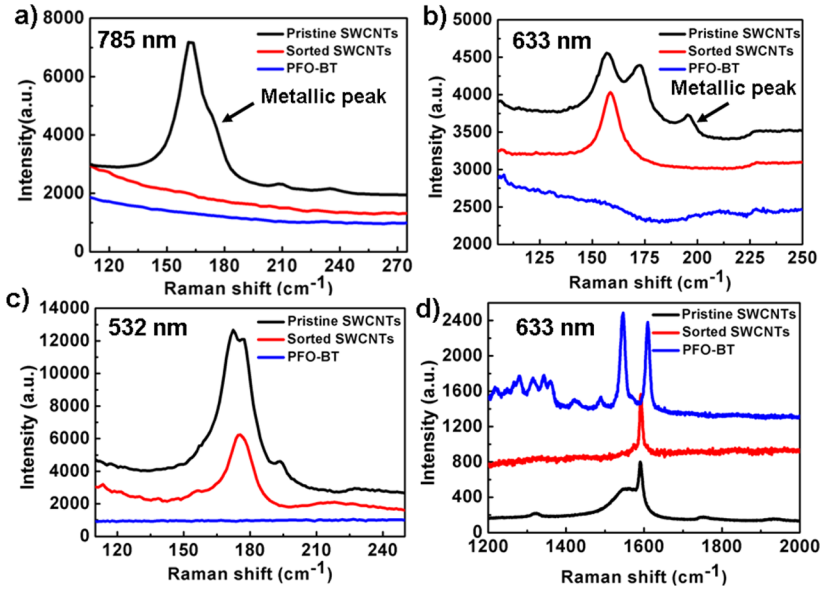

Figure 2. Raman spectra of pristine SWCNTs, PFO-BT, and SWCNTs sorted by PFO-BT under (a) 785 nm, (b, d) 633 nm, and (c) 532 nm lasers.

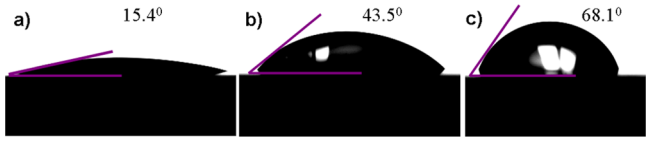

Figure 3. Water contact angles of three SiO_2/Si substrates: (a) substrates after oxygen plasma treatment, (b) untreated substrates, and (c) substrates after being annealed at 200 °C in a vacuum oven for 1 h.

substrates, respectively. Furthermore, the devices showed a small hysteresis and low operation voltage.

The detailed structures of sc-SWCNTs at different sites in different device channels were characterized by AFM. Figure 5 and Figures S2−S4 in the Supporting Information give the typical AFM images of the SWCNT thin film on substrates with different water contact angles. As shown in Figures 5 and S2−S4, the diameters of sorted sc-SWCNTs are in the range of 1.3−1.6 nm, indicating that the SWCNT thin films consist of individual SWCNTs and a few small SWCNT bundles, and the lengths of individual SWCNTs are about 1−3 μm. As evident, the density of SWCNTs in the channels depends on the wettability of the substrates. More hydrophilic substrates resulted in a higher density of SWCNTs. The density is estimated to be about 3, 8, and 35 SWCNTs/μm^2 for substrates with water contact angles of 68.1°, 43.5° and 15.4°, respectively. Furthermore, as shown in Figure 4, p-type TFTs are gating at +10 V. This is probably due to the fact that the wrapped PFO-BT acts as a hole dopant, resulting in the

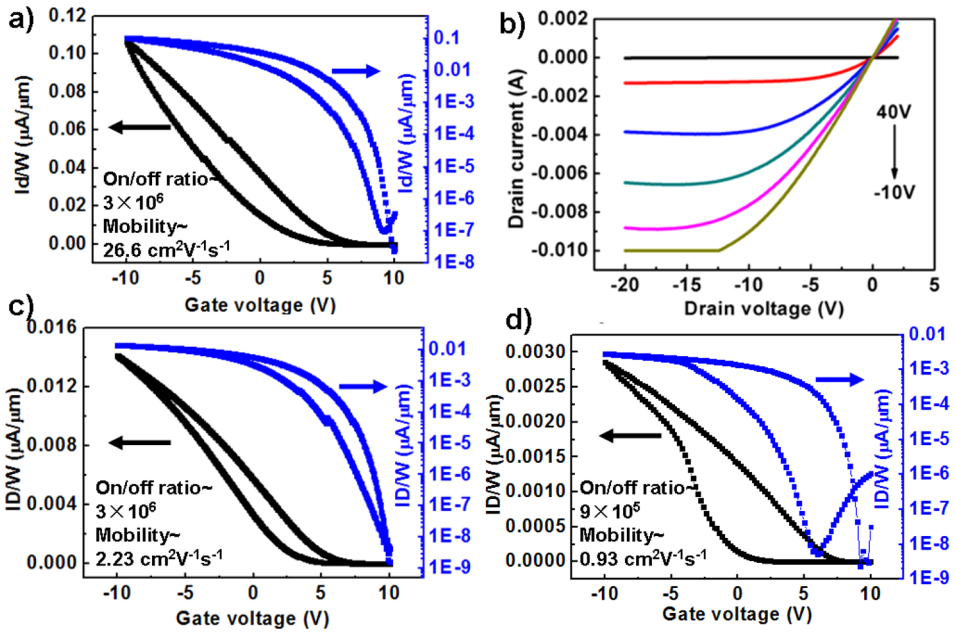

Figure 4. Typical transfer and output characteristics of TFTs based on sc-SWCNTs sorted from arc discharge SWCNTs. (V_{ds} = 1 V): (a, b) substrates treated with oxygen plasma for 1 min, (c) untreated substrates, and (d) substrates annealed at 200 °C for 1 h.

dx.doi.org/10.1021/am502168x | ACS Appl. Mater. Interfaces 2014, 6, 9997−10004

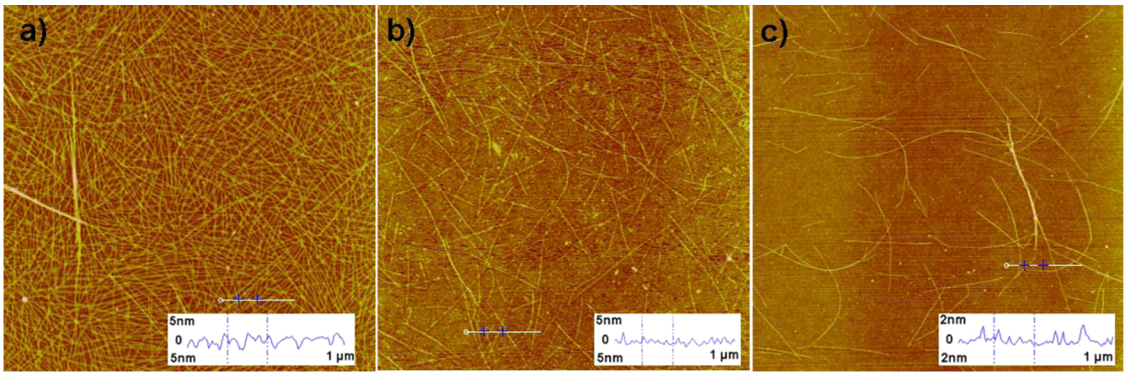

Figure 5. Typical AFM images of sorted SWCNTs in the device channels with different treatments: (a) oxygen plasma treatment for 1 min, (b) without any treatment, and (c) annealing at 200 °C for 1 h (the white scale bar is 1 μm).

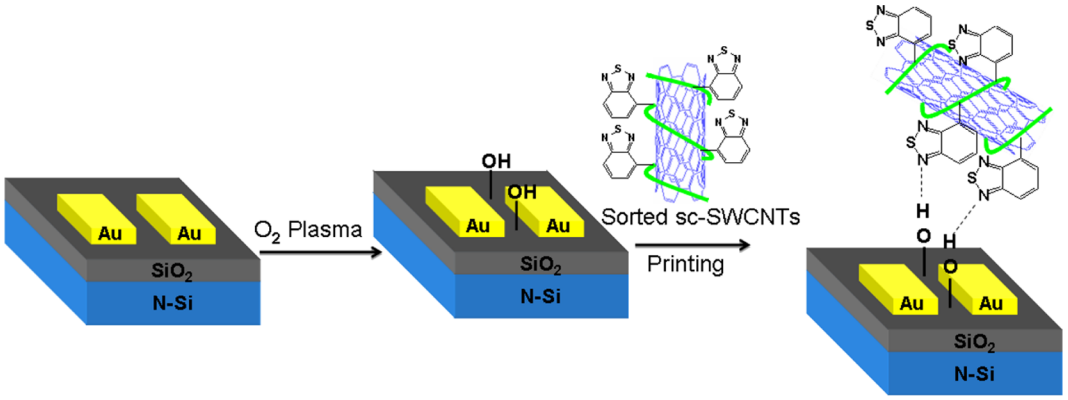

Figure 6. Schematic of the immobilization of sc-SWCNTs sorted by PFO-BT on the oxygen plasma treated substrate via hydrogen bonds.

threshold voltages of SWCNT TFTs being shifted to positive gate voltages.

A possible mechanism for immobilizing sc-SWCNTs on hydroxyl-functionalized substrates was proposed as illustrated in Figure 6. The hydroxyl monolayer on the SiO_2/Si substrate is formed after oxygen plasma treatment. sc-SWCNTs sorted by PFO-BT, which contains nitrogen atoms with high electronegativity in 1,4-benzo-2,1,3-thiadiazole, can be easily immobilized on hydroxyl-functionalized substrates due to the formation of a hydrogen bond between the hydroxyl groups and nitrogen atom in 1,4-benzo-2,1,3-thiadiazole. To verify our proposed hypothesis, X-ray photoelectron spectroscopy (XPS) of SiO_2 substrates was carried out. Figure 7 shows the O 1s XPS spectra of the untreated SiO_2 and oxygen plasma treated SiO_2 with and without PFO-BT-sorted sc-SWCNTs. As shown in Figure 7, the O 1s peaks shifted from 533.28 to 533.11 eV; at the same time, the height of the O 1s peaks increased after treatment with oxygen plasma, which was ascribed to increased amounts of SiOH groups on the SiO_2 substrates. After immobilization of sc-SWCNTs on oxygen plasma treated substrates, the O 1s peaks shifted to a lower binding energy (532.49 eV) due to hydrogen bonding.[43] As described above, the O 1s XPS data support our hypothesis. Furthermore, the influence of the oxygen plasma treatment time on the electrical properties of TFTs was also studied. As shown in Figure S5 (Supporting Information), the mobility and on/off ratio of TFTs had no obvious differences when the oxygen plasma treatment time was extended to 5 and 10 min, which demonstrated that the number of hydroxyl groups on the substrates after oxygen plasma treatment for 1 min was enough for immobilizing sc-SWCNTs. To obtain high-performance TFTs, all substrates were treated with oxygen plasma for 1 min prior to deposition of SWCNTs in the following experiments.

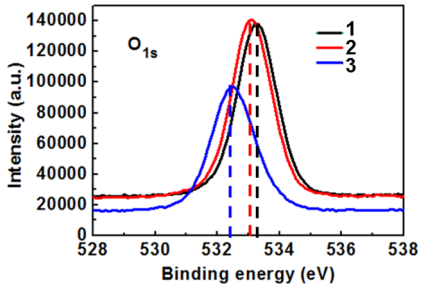

Figure 7. O 1s XPS spectra of SiO_2 substrates: (1) untreated and oxygen plasma treated $SiO_2$and (2) SiO_2 without and (3) with PFO-BT-sorted sc-SWCNTs.

To demonstrate oxygen plasma treatment for improving the uniformity of printed SWCNT TFTs, TFT arrays consisting of 200 devices were fabricated by aerosol-jet-printing on oxygen plasma treated substrates. As-prepared sc-SWCNT inks were selectively deposited in the channels of 200 devices by aerosol-jet-printing; after that, the devices were washed three times with xylene to remove impurities. As shown in Figure 8, printed TFTs showed excellent performance and uniformity. On currents and mobilities are in the ranges of (0.75−3.65) × 10^{-4} A and (8.2−32.3) cm^2 V^{-1} s^{-1}, respectively. It is noted that the mobilities of 85% printed devices are in the range of 12−20 cm^2 V^{-1} s^{-1}. On/off ratios of 179 devices are in the range of 10^5−10^8, and only 9 and 11 devices showed on/off

dx.doi.org/10.1021/am502168x | ACS Appl. Mater. Interfaces 2014, 6, 9997−10004

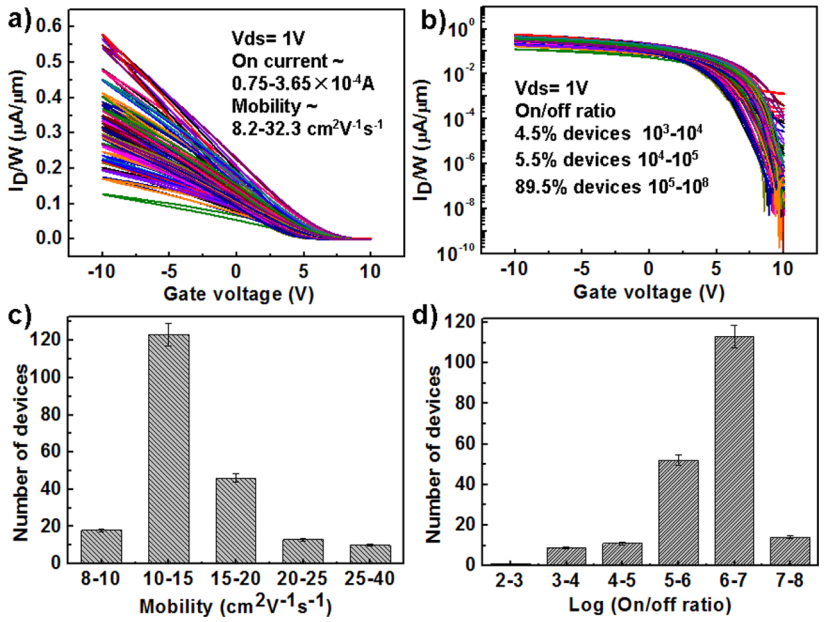

Figure 8. Transfer characteristic curves of the same printing batch of 200 devices on oxygen plasma treated SiO_2/Si substrates: (a) linear scale and (b) log scale. Histograms of the (c) mobility and (d) on/off ratios of 200 printed TFTs.

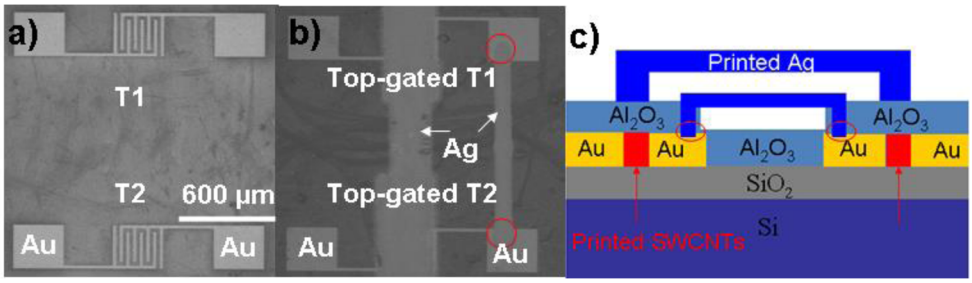

Figure 9. (a) Optical images of two pairs of gold interdigitated electrodes after SWCNTs are printed. (b) Printed inverter based on printed top-gate transistors. (c) Schematic of a printed inverter on SiO_2/Si substrates. T1 and T2 represent printed transistor 1 and transistor 2, respectively. Red circles in (b) and (c) represent the connection points of printed silver electrodes and gold electrodes.

ratios in the ranges of 10^3-10^4 and 10^4-10^5, respectively. Table S1 (Supporting Information) lists the electrical properties and some important parameters of SWCNT TFTs reported by several groups. As shown in Table S1, our printed TFTs showed a higher on/off ratio with high mobility.

Xylene is a volatile organic compound, and it volatilizes rapidly once sc-SWCNT inks are printed on substrates. As described above, high-density SWCNTs were observed in the channel after only two printings, which demonstrated that PFO-BT-functionalized sc-SWCNTs could react rapidly with hydroxyl groups on the substrates to form hydrogen bonds and then become immobilized on the substrates. To test the adhesion force between PFO-BT-functionalized sc-SWCNTs and the oxygen plasma treated substrates, printed TFTs were placed in xylene and then sonicated (40 W, 59 kHz) for 5, 15, and 45 min. As shown in Figure S6 (Supporting Information), on/off ratios have no changes after sonication treatment for 45 min. Although the mobility gradually decreases with increasing sonication time, the mobility is reduced only 20% after sonication in a water bath for 45 min, indicating the adhesive force is strong between PFO-BT-functionalized sc-SWCNTs and the substrates.

Fabrication and Characterization of Printed Inverters Based on Printed Top-Gate SWCNT TFTs. Inverters composed of two top-gate TFTs were fabricated on a SiO_2/Si substrate using Al_2O_3 as the dielectric layer and printed silver electrodes as the top-gate electrodes. Parts a and b of Figure 9 show the pictures of two pairs of gold electrodes and an inverter with two top-gate printed TFTs, and the schematic structure of an inverter containing two printed top-gate TFTs is shown in Figure 9c. The transfer characteristics of the bottom-gate TFTs have been measured before and after deposition of an Al_2O_3 thin film on top of the SWCNT thin film. As shown in Figure 10a, the mobilities of the two bottom-gate transistors are 19.5 and 17.4 $cm^2\ V^{-1}\ s^{-1}$, and the on/off ratios are 4×10^6 and 4×10^6, respectively. However, all of them showed ambipolar characteristics with slightly pronounced n-type conduction after deposition of Al_2O_3 at 200 °C, and the mobilities and on/off ratios of the transistors decreased to about 1.4 $cm^2\ V^{-1}\ s^{-1}$ and 4×10^3 due to the formation of defects on the carbon nanotube surfaces by atomic layer deposition (ALD) precursors.[44,45] Interestingly, the channel conduction of the printed top-gate transistors showed slightly ambipolar characteristics with strong n-type conduction after the silver electrodes were printed on top of the bottom device channels (Figure 10b). As shown in Figure 10b, when the gate voltages were larger than 1 V, the printed top-gate TFTs displayed n-type conduction, which is in agreement with the previous work.[44] The mobilities and on/off

dx.doi.org/10.1021/am502168x | ACS Appl. Mater. Interfaces 2014, 6, 9997−10004

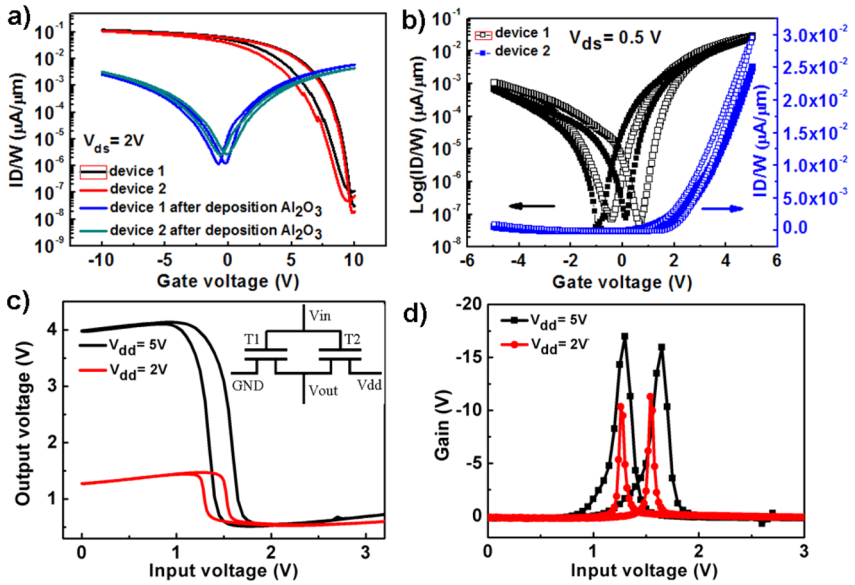

Figure 10. (a) Transfer curves of two transistors on prepatterned interdigitated gold electrodes on SiO_2/Si substrates before and after deposition of 70 nm Al_2O_3 by ALD at 200 °C (V_{ds} = 2 V). (b) Transfer curves of printed top-gate devices 1 and 2 with log and linear scales (V_{ds} = 0.5 V). (c) Input−output and (d) gain characteristics of an inverter at V_{dd} = 5 and 2 V. The value of the gain is 17 and 11, respectively. The inset shows a diagram of an inverter. T1 and T2 represent printed transistor 1 and transistor 2, respectively.

ratios of printed top-gate TFTs can be up to 4.6 cm^2 V^{-1} s^{-1} and 4 × 10^5, respectively. This is probably attributed to an increase in the contact areas between the SWCNT thin film and dielectric layers in printed top-gate TFTs, inducing more electronic carriers. Parts c and d of Figure 10 show the voltage input−output characteristics of the inverter, which exhibited a maximum voltage gain of 17 and 11 at V_{dd} = 5 and 2 V, respectively. As shown in Figure 10c, when the input voltage is "high" (greater than 1.8 V), transistor 1 is in the on state and transistor 2 operates in the quasi-off state, resulting in a "low" output voltage. Since transistor 1 goes into the off state and transistor 2 operates in the on state as the input voltage decreases (about 1.6 V), the reverse is observed. To eliminate the influence of ALD precursors, we are trying to introduce a buffer layer in the middle of the SWCNT thin film and Al_2O_3 thin film to protect sc-SWCNTs. It has been found that parylene shows excellent compatibility with SWCNTs. As shown in Figure S7 (Supporting Information), both the mobility and on/off ratio have no changes after deposition of parylene on top of the SWCNT thin film due to the low reactivity of parylene precursor molecules.

EXPERIMENTAL SECTION

Materials and Instruments. Arc discharge (P2, diameter 1.2−1.6 nm) SWCNTs were purchased from Carbon Solutions. PFO-BT (M_w = 21 000 g mol^{-1}) was purchased from Shenzhen (China) Derthon Optoelectronic Materials Science & Technology. Conducting nanosilver inks were purchased from the Beijing Institute of Graphic Communication. All products were directly used without further purifications. A confocal Raman microscope (WITec CRM200) equipped with 785, 633, and 532 nm lasers was used for Raman measurements. Optical absorption measurements were performed with a PerkinElmer Lambda 750 UV−vis−NIR spectrometer. All electrical measurements were carried out in ambient conditions using a Keithley semiconductor parameter analyzer (model 4200-SCS). An NSCRIPTOR DPN system (NanoInk Inc., Skokie, IL) and Dimension 3100 atomic force microscope (Veeco, Santa Clara, CA) were used for AFM imaging. Sorted sc-SWCNT solutions and nanosilver inks were printed with an aerosol Jet 300P system (Optomec Inc., United States). The contact angle was measured by using a contact angle setup (OCA20, Data Physics Germany). X-ray photoelectron spectroscopy (XPS) analysis was performed with an ESCA Lab 220I-XL using Al Kα radiation.

Preparation of sc-SWCNT Inks. To prepare sc-SWCNT inks, 2 mg of arc discharge SWCNTs was dispersed in 15 mL of xylene with 9 mg of PFO-BT via probe ultrasonication for 30 min (Sonics & Materials Inc., model VCX 130, 60 W). Then the resulting SWCNT solutions were centrifuged at 21000g for 30 min to remove metallic species and big bundles, and the supernatant was drawn out from the centrifuge tube and used to fabricate SWCNT TFTs without any other purification.

Fabrication and Electrical Properties of Printed SWCNT TFTs. To assess the quality of sorted sc-SWCNT inks, they were deposited on prepatterned interdigitated gold electrodes (with different fingers by photolithography; the finger dimensions were 1000 or 200 μm width, 20 μm length, and 20 μm interfinger spacing) on oxygen plasma treated SiO_2 (the thickness is 300 nm)/Si substrates by both aerosol-jet-printing and drop-casting. For the printing process, sorted SWCNT solutions were printed onto the channels of pretreated devices, followed by washing with xylene three times. The printing procedure was only repeated two times, and the density of sorted sc-SWCNTs was high enough to form a percolation path and to reach the desired current level. The details of the printing conditions are listed as follows: SWCNT inks were atomized to form aerosols by sonication at a power of 25 W. The sheath gas flow and atomizer flow were 50 and 20 cm^3, respectively. The printing speed was 0.5 mm s^{-1}. The nozzle size of the printed head was 150 μm. All operations were at room temperature. For the drop-casting procedure, 15 μL of sorted sc-SWCNT solutions were dropped onto prepatterned interdigitated gold electrodes, followed by drying at room temperature and rinsing with xylene three times. The procedure was repeated four times. After that, the devices were dipped into hot xylene for 30 min to further remove the residual polymers.

To obtain top-gate TFTs with independently controlled gates, sorted sc-SWCNT inks were first printed on prepatterned interdigitated gold electrodes on SiO_2/Si substrates. After that, 70 nm thick Al_2O_3 thin films were deposited on top of predeposited SWCNT thin films at 200 °C by atomic layer deposition (ALD) (Cambridge NanoTech Inc.). Then, silver top-gate electrodes were printed on the top of gold electrodes by aerosol-jet-printing. Holes were created in the Al_2O_3 thin films using the probe needle. Finally,

two top-gate TFTs were connected with printed silver lines, and the inverter was ready to use.

The electrical properties of SWCNT TFTs were measured at room temperature. The mobilities of SWCNT TFTs are estimated by $\mu = (dI_d/dV_g)(L/W)(1/C_iV_{ds})$.[13,14] Here, C_i is the oxide capacitance per unit area and L and W represent the channel length and width, respectively.

CONCLUSIONS

In summary, deposition of high-density sc-SWCNTs can be achieved by tuning the wettability of SiO_2/Si substrates. The density of SWCNTs and electrical properties of SWCNT TFTs increased with decreasing water contact angle of the substrates. Printed TFTs exhibited good uniformity and excellent electrical properties with high mobility, a high on/off ratio, a low operation voltage, and a small hysteresis. Printed top-gate TFTs with slightly ambipolar characteristics and strong n-type conduction were obtained using ALD of Al_2O_3 thin films as the dielectric layer and printed silver electrodes as the top-gate electrodes by aerosol-jet-printing. Printed inverters based on the printed top-gate TFTs showed voltage gains of up to 17 and 11 at V_{dd} = 5 and 2 V, respectively.

ASSOCIATED CONTENT

Supporting Information

Effect of APTES and poly-L-lysine on the electrical properties of TFTs, AFM images of SWCNTs on substrates with different water contact angles, effect of the oxygen plasma treatment time on the electrical properties of TFTs, binding force test of printed TFTs, effect of parylene on the electrical properties of TFTs, and comparison of the electrical properties of TFTs reported by several groups. This material is available free of charge via the Internet at http://pubs.acs.org.

AUTHOR INFORMATION

Corresponding Authors

*E-mail: jwzhao2011@sinano.ac.cn.

*E-mail: zcui2009@sinano.ac.cn.

Notes

The authors declare no competing financial interest.

ACKNOWLEDGMENTS

This work was supported by the National Natural Science Foundation of China (Grants 91123034 and 61102046), the Knowledge Innovation Programme of the Chinese Academy of Sciences (Grant KJCX2-EW-M02), and the Basic Research Programme of Jiangsu Province (Grant BK2011364).

REFERENCES

(1) Vaillancourt, J.; Zhang, H. Y.; Vasinajindakaw, P.; Xia, H. T.; Lu, X. J.; Han, X. L.; Chen, R. T.; Berger, U.; Renn, M. All Ink-Jet-Printed Carbon Nanotube Thin-film Transistor on a Polyimide Substrate with an Ultrahigh Operating Frequency of Over 5 GHz. *Appl. Phys. Lett.* **2008**, *93*, 243301−243303.

(2) Gracia-Espino, E.; Sala, G.; Pino, F.; Halonen, N.; Luomahaara, J.; Maklin, J.; Kords, K.; Vajtai, R. Electrical Transport and Field-Effect Transistors Using Inkjet-Printed SWCNT Films Having Different Functional Side Groups. *ACS Nano* **2010**, *4*, 3318−3324.

(3) Noh, J.; Jung, M.; Jung, K.; Lee, G.; Kim, J.; Lim, S.; Kim, D.; Choi, Y.; Kim, Y.; Subramanian, V.; Cho, G. Fully Gravure-Printed D Flip-Flop on Plastic Foils Using Single-Walled Carbon Nanotube Based TFTs. *IEEE Trans. Electron Devices* **2011**, *32*, 638−640.

(4) Jung, M.; Kim, J.; Noh, J.; Lim, N.; Lim, C.; Lee, G.; Kim, J.; Kang, H.; Jung, K.; Leonard, A. D.; Tour, J. M.; Cho, G. All-Printed and Roll-to-Roll Printable 13.56-MHz-Operated 1-Bit RF Tag on Plastic Foils. *IEEE Trans. Electron Devices* **2010**, *57*, 571−580.

(5) Cho, J. H.; Lee, J. Y.; Xia, Y.; Kim, B.; He, Y. Y.; Renn, M. J.; Lodge, T. P.; Frisbie, C. D. Printable Ion-Gel Gate Dielectrics for Low-Voltage Polymer Thin-Film Transistors on Plastic. *Nat. Mater.* **2008**, *7*, 900−906.

(6) Kim, M. G.; Kanatzidis, M. G.; Facchetti, A.; Marks, T. J. Low-Temperature Fabrication of High-Performance Metal Oxide Thin-Film Electronics via Combustion Processing. *Nat. Mater.* **2011**, *10*, 382−388.

(7) Zhao, Y.; Di, C.; Gao, X.; Hu, Y.; Guo, Y.; Zhang, L.; Liu, Y.; Wang, J.; Hu, E.; Zhu, D. All Solution-Processed, High-Performance n-Channel Organic Transistors and Circuits: Toward Low-Cost Ambient Electronics. *Adv. Mater.* **2011**, *23*, 2448−2453.

(8) Ng, T. N.; Schwartz, D. E.; Lavery, L. L.; Whiting, G. L.; Russo, B.; Krusor, B.; Veres, J.; Bröms, P.; Herlogsson, L.; Alam, N.; Hagel, O.; Nilsson, J.; Karlsson, C. Scalable Printed Electronics: An Organic Decoder Addressing Ferroelectric Non-Volatile Memory. *Sci. Rep.* **2012**, *2* (585), 1−7.

(9) Wang, C.; Takei, A. K.; Takahashiab, A. T.; Javey, A. Carbon Nanotube Electronics—Moving Forward. *Chem. Soc. Rev.* **2013**, *42*, 2592−2609.

(10) Ha, M. J.; Seo, J. W. T.; Prabhumirashi, P. L.; Zhang, W.; Geier, M. L.; Renn, M. J.; Kim, C. H.; Hersam, M. C.; Frisbie, C. D. Aerosol 10 Jet Printed, Low Voltage, Electrolyte Gated Carbon Nanotube Ring Oscillators with Sub-5μs Stage Delays. *Nano Lett.* **2013**, *13*, 954−960.

(11) Lau, P. H.; Takei, K.; Wang, C.; Ju, Y.; Kim, J.; Yu, Z. B.; Takahashi, T.; Cho, G.; Javey, A. Fully Printed, High Performance Carbon Nanotube Thin-Film Transistors on Flexible Substrates. *Nano Lett.* **2013**, *13*, 3864−3869.

(12) Hong, K.; Kim, S. H.; Lee, K. H.; Frisbie, C. D. Printed, Sub-2V ZnO Electrolyte Gated Transistors and Inverters on Plastic. *Adv. Mater.* **2013**, *25*, 3413−3418.

(13) Sun, D.; Timmermans, M. Y.; Tian, Y.; Nasibulin, A. G.; Kauppinen, E. I.; Kishimoto, S.; Mizutani, T.; Nat, Y. O. Length-Sorted Semiconducting Carbon Nanotubes for High-Mobility Thin Film Transistors. *Nat. Nanotechnol.* **2011**, *6*, 156−161.

(14) Sun, D. M.; Timmermans, M. Y.; Kaskela, A.; Nasibulin, A. G.; Kishimoto, S.; Mizutani, T.; Kauppinen, E. I.; Ohno, Y. Mouldable All-Carbon Integrated Circuits. *Nat. Commun.* **2013**, *4*, 2302.

(15) Xu, W. Y.; Zhao, J. W.; Qian, L.; Han, X. Y.; Wu, L. Z.; Wu, W. C.; Song, M. S.; Zhou, L.; Su, W. M.; Wang, C.; Nie, S. H.; Cui, Z. Sorting of Large-Diameter Semiconducting Carbon Nanotube and Printed Flexible Driving Circuit for Organic Light Emitting Diode (OLED). *Nanoscale* **2014**, *6*, 1589−1595.

(16) Chen, P.; Fu, Y.; Aminirad, R.; Wang, C.; Zhang, J. L.; Wang, K.; Galatsis, K.; Zhou, C. W. Fully Printed Separated Carbon Nanotube Thin Film Transistor Circuits and Its Application in Organic Light Emitting Diode Control. *Nano Lett.* **2011**, *11*, 5301−5308.

(17) Ishikawa, F. N.; Chang, H. K.; Ryu, K.; Chen, P. C.; Badmaev, A.; Arco, L. G.D.; Shen, G. Z.; Zhou, C. W. Transparent Electronics Based on Transfer Printed Aligned Carbon Nanotubes on Rigid and Flexible Substrates. *ACS Nano* **2008**, *3*, 73−79.

(18) Takei, K.; Takahashi, T.; Ho, J. C.; Ko, H.; Gillies, A. G.; Leu, P. W.; Fearing, R. S.; Javey, A. Nanowire Active-Matrix Circuitry for Low-Voltage Macroscale Artificial Skin. *Nat. Mater.* **2010**, *9*, 821−826.

(19) Takahashi, T.; Takei, K.; Gillies, A. G.; Fearing, R. S.; Javey, A. Carbon Nanotube Active-Matrix Backplanes for Conformal Electronics and Sensors. *Nano Lett.* **2011**, *11*, 5408−5413.

(20) Wang, C.; Qian, L.; Xu, W. Y.; Nie, S. H.; Gu, W. B.; Zhang, J. H.; Zhao, J. W.; Lin, J.; Chen, J.; Cui, Z. High Performance Thin Film Transistors Based on Regioregular Poly(3-dodecylthiophene)-Sorted Large Diameter Semiconducting Single-Walled Carbon Nanotubes. *Nanoscale* **2013**, *5*, 4156−4161.

(21) Qian, L.; Xu, W. Y.; Fan, X. F.; Wang, C.; Zhang, J. H.; Zhao, J. W.; Cui, Z. Electrical and Photoresponse Properties of Printed Thin-Film Transistors Based on Poly(9,9-dioctylfluorene-*co*-bithiophene) Sorted Large-Diameter Semiconducting Carbon Nanotubes. *J. Phys. Chem. C* **2013**, *117*, 18243−18250.

(22) Zhao, J. W.; Gao, Y. L.; Gu, W. B.; Wang, C.; Lin, J.; Chen, Z.; Cui, Z. Fabrication and Electrical Properties of All-Printed Carbon Nanotube Thin Film Transistors on Flexible Substrates. *J. Mater. Chem.* **2012**, *22*, 20747−20753.
(23) Lee, H. W.; Yoon, Y. H.; Park, S.; Oh, J. H.; Hong, S. H.; Liyanage, L. S.; Wang, H. L.; Morishita, S.; Patil, N.; Park, Y. J.; Spakowitz, A.; Galli, G.; Gygi, F.; Wong, P. H.-S.; Tok, J. B.-H.; Kim, J. M.; Bao, Z. N. Selective Dispersion of High Purity Semiconducting Single-Walled Carbon Nanotubes with Regioregular Poly(3-alkylthiophene)s. *Nat. Commun.* **2011**, *2*, 541−258.
(24) Wang, H. L.; Mei, J. G.; Liu, P.; Schmidt, K.; Jiménez-Osés, K.; Osuna, S.; Fang, L.; Tassone, C. J.; Zoombelt, A. P.; Sokolov, A. N.; Houk, K. N.; Toney, M. F.; Bao, Z. N. Scalable and Selective Dispersion of Semiconducting Arc-Discharged Carbon Nanotubes by Dithiafulvalene/Thiophene Copolymers for Thin Film Transistors. *ACS Nano* **2013**, *7*, 2659−2668.
(25) Liu, Z. Y.; Qiu, Z. J.; Zhang, S. L.; Zhang, Z. B. Small-Hysteresis Thin-Film Transistors Achieved by Facile Dip-Coating of Nanotube/Polymer Composite. *Adv. Mater.* **2012**, *24*, 3633−3638.
(26) Harris, J. M.; Swathi Iyer, G. R.; Bernhardt, A. K.; Huh, J. Y.; Hudson, S. D.; Fagan, J. A.; Hobbie, E. K. Electronic Durability of Flexible Transparent Films from Type-Specific Single-Wall Carbon Nanotubes. *ACS Nano* **2012**, *6*, 881−887.
(27) Khripin, C. Y.; Fagan, J. A.; Zheng, M. Spontaneous Partition of Carbon Nanotubes in Polymer-Modified Aqueous Phases. *J. Am. Chem. Soc.* **2013**, *135*, 6822−6825.
(28) Gerstel, P.; Klumpp, S.; Hennrich, F.; Poschlad, A.; Meded, V.; Blasco, E.; Wenzel, W.; Kappes, M. M.; Kowollik, C. B. Highly Selective Dispersion of Single-Walled Carbon Nanotubes via Polymer Wrapping: A Combinatorial Study via Modular Conjugation. *ACS Macro Lett.* **2014**, *3*, 10−15.
(29) Sundramoorthy, A. K.; Mesgari, S.; Wang, J.; Kumar, Raj.; Sk, M. A.; Yeap, S. H.; Zhang, Q.; Sze, S. K.; Lim, K. H.; Chan-Park, M. B. Scalable and Effective Enrichment of Semiconducting Single-Walled Carbon Nanotubes by a Dual Selective Naphthalene-Based Azo Dispersant. *J. Am. Chem. Soc.* **2013**, *135*, 5569−5581.
(30) Kim, D. H.; Shin, H. J.; Lee, H. S.; Lee, J.; Lee, B. L.; Lee, W. H.; Lee, J. H.; Cho, K.; Kim, W.; Lee, S. Y.; Choi, J.; Kim, J. M. Designing Nanoparticle Translocation through Membranes by Computer Simulations. *ACS Nano* **2012**, *6*, 662−670.
(31) Mistry, K. S.; Larsen, B. A.; Blackburn, J. L. High-Yield Dispersions of Large-Diameter Semiconducting Single-Walled Carbon Nanotubes with Tunable Narrow Chirality Distributions. *ACS Nano* **2013**, *7*, 2231−2239.
(32) Mesgari, S.; Poon, Y. F.; Leslie, S.; Chan-Park, M. B. High Selectivity cum Yield Gel Electrophoresis Separation of Single-Walled Carbon Nanotubes Using a Chemically Selective Polymer Dispersant. *J. Phys. Chem. C* **2012**, *116*, 10266−10273.
(33) Arnold, M. S.; Green, A. A.; Hulvat, J. F.; Stupp, S. I.; Hersam, M. C. Sorting Carbon Nanotubes by Electronic Structure Using Density Differentiation. *Nat. Nanotechnol.* **2006**, *1*, 60−65.
(34) Wu, J.; Hong, G. S.; Lim, H. E.; Thendie, B.; Miyata, Y.; Shinohara, H.; Dai, H. J. Short Channel Field-Effect Transistors from Highly Enriched Semiconducting Carbon Nanotubes. *Nano Res.* **2012**, *5*, 388−394.
(35) Miyata, Y.; Shiozawa, K.; Asada, Y.; Ohno, Y.; Kitaura, R.; Mizutani, T.; Shinohara, H. Length-Sorted Semiconducting Carbon Nanotubes for High-Mobility Thin Film Transistors. *Nano Res.* **2011**, *4*, 963−970.
(36) Wang, C.; Zhang, J.; Ryu, K.; Badmaev, A.; Gomez, L.; Zhou, C. Wafer-Scale Fabrication of Separated Carbon Nanotube Thin-Film Transistors for Display Applications. *Nano Lett.* **2009**, *9*, 4285−4291.
(37) Takahashi, T.; Takei, K.; Gillies, A. G.; Fearing, R. S.; Javey, A. Carbon Nanotube Active-Matrix Backplanes for Conformal Electronics and Sensors. *Nano Lett.* **2011**, *11*, 5408−5413.
(38) Wang, C.; Chien, J. C.; Takei, K.; Takahashi, T.; Nah, J.; Niknejad, A. M.; Javey, A. High-Performance Integrated Circuits Using Semiconducting Carbon Nanotube Networks for Digital, Analog, and Radio-Frequency Applications. *Nano Lett.* **2012**, *12*, 1527−1533.
(39) Park, H.; Afzali, A.; Han, S. J.; Tulevski, G. S.; Franklin, A. D.; Tersoff, J.; Hannon, J. B.; Haensch, W. High-Density Integration of Carbon Nanotubes via Chemical Self-Assembly. *Nat. Nanotechnol.* **2012**, *7*, 787−791.
(40) Zhao, J. W.; Qian, J.; Shen, Y. Q.; Wang, X. H.; Shi, A. H.; Lee, C. W. High Yield Fabrication of Semiconducting Thin-Film Field-Effect Transistors Based on Chemically Functionalized Single-Walled Carbon Nanotubes. *Sci. China: Chem.* **2011**, *54*, 1484−1490.
(41) Tanaka, T.; Jin, H.; Miyata, Y.; Fujii, S.; Suga, H.; Naitoh, Y.; Minari, T.; Miyadera, T.; Tsukagoshi, K.; Kataura, H. Simple and Scalable Gel-Based Separation of Metallic and Semiconducting Carbon Nanotubes. *Nano Lett.* **2009**, *9*, 1497−1500.
(42) Liu, H. P.; Nishide, D.; Tanaka, T.; Kataura, H. Large-Scale Single-Chirality Separation of Single-Walled Carbon Nanotubes by Simple Gel Chromatography. *Nat. Commun.* **2011**, *2*, 309.
(43) Li, L.; Chan, C. M.; Weng, L. T. Surface Study of Poly(vinyl alcohol) and Poly(N-vinyl-2-pyrrolidone) Miscible Blends. *Annual Technical Conference—ANTEC, Conference Proceedings*; Society of Plastics Engineers: Newtown, CT, 1997; Vol. 2, p 2531.
(44) Zhang, J. L.; Wang, C.; Fu, Y.; Che, Y.; Zhou, C. W. Air-Stable Conversion of Separated Carbon Nanotube Thin-Film Transistors from p-Type to n-Type Using Atomic Layer Deposition of High-κ Oxide and Its Application in CMOS Logic Circuits. *ACS Nano* **2011**, *5*, 3284−3292.
(45) Grigoras, K.; Zavodchikova, M. Y.; Nasibulin, A. G.; Kauppinen, E. I.; Ermolov, V.; Franssila, S. J. Atomic Layer Deposition of Aluminum Oxide Films for Carbon Nanotube Network Transistor Passivation. *J. Nanosci Nanotechnol.* **2011**, *11*, 8818−8825.